Electronic Supplementary Material (ESI) for Green Chemistry.

Supporting information

Controlling the toxicity of biomass-derived difunctional molecules as potential pharmaceutical ingredients for specific activity toward microorganisms and mammalian cells

Hochan Chang[‡a], Douglas H. Chang[‡a], Alexios G. Stamoulis[b], George W. Huber[a], David M. Lynn[a,b], Sean P. Palecek[a], James A. Dumesic[a,c]*

[a]Department of Chemical and Biological Engineering, University of Wisconsin–Madison, Madison, WI, USA.

[b]Department of Chemistry, University of Wisconsin–Madison, Madison, WI, USA.

[c]DOE Great Lakes Bioenergy Research Center, University of Wisconsin–Madison, Madison, WI, USA

[‡]These authors contributed equally.

*Corresponding author. E-mail: jdumesic@wisc.edu

General considerations for experimental methods

Chromatography separation of Diels-Alder adducts. The purification of the Diels-Alder adducts was performed via column chromatography on a Biotage Isolera One unit with the aid of 40 g RediSep Gold normal phase column. The separations were performed on 500 mg portions of crude material utilizing a dichloromethane/methanol mobile phase flowed at 100 mL/min. The mobile phase was kept at 1% methanol for 3 column volumes (CVs), then swept to 10% methanol over 8 column volumes, followed by an isocratic region at 10% methanol for 3 column volumes.

HPLC analysis for quantification of chemical concentrations. The chemical concentrations of the samples from the reaction kinetics experiments were measured by high performance liquid chromatography (HPLC) analysis. 0.2 g (200 µL) of sample was diluted in 0.2 g (200 µL) of MQ water (2 times dilution by volume), and the diluted samples were filtered by syringe filter (20 µm pore) to analyze the concentrations of N-substituted maleimides (EMAL, 3-Maleimidopropionic acid) and the Diels-Alder adducts (Entry 4,7). The concentrations of the Diels-Alder adducts (Entry 4,7) in aqueous solution were measured by a Water 2695 separation module equipped with an Aminex HPX-87H (Bio-Rad) column and a Waters 2998 PDA detector, set at 210 nm, while the concentrations of N-substituted maleimides (EMAL, 3-Maleimidopropionic acid) were measured with the PDA detector, set at 310 nm. The temperature of the HPLC column was maintained at 50℃, and the flow rate of the mobile phase (pH 2 water, acidified by sulfuric acid) was 0.6 mL/min.

NMR analysis for the compounds. ^{13}C quantitative nuclear magnetic resonance (qNMR), and 2D HSQC NMR spectra were obtained using a Brucker Avance-500 spectrometer. Tetramethylsilane (TMS) (δ: 0 ppm) or deuterated solvents (e.g. MeOD, CDCl3, DMSO-d6) were used as a reference for chemical shifts.

General considerations for toxicity assays. *Candida spp.* cells were streaked on a yeast peptone dextrose (YPD) agar plate from a frozen stock solution and grown overnight at 30°C. For each assay, a colony was collected from the YPD plate and grown overnight in 15 mL centrifuge tubes at 30°C in liquid YPD broth, and cells were then washed, resuspended, and prepared for subsequent experiments. *S. aureus* cells were maintained in a similar fashion but on trypsin-soy agar plates from frozen stock. For time-kill experiments, *C. albicans* colonies on agar plates were counted manually. Absorbance measurements used in XTT assays were acquired at 490 nm using a plate reader (EL800 Universal Microplate Reader, Bio-Tek Instruments, Inc).

Figures and Tables

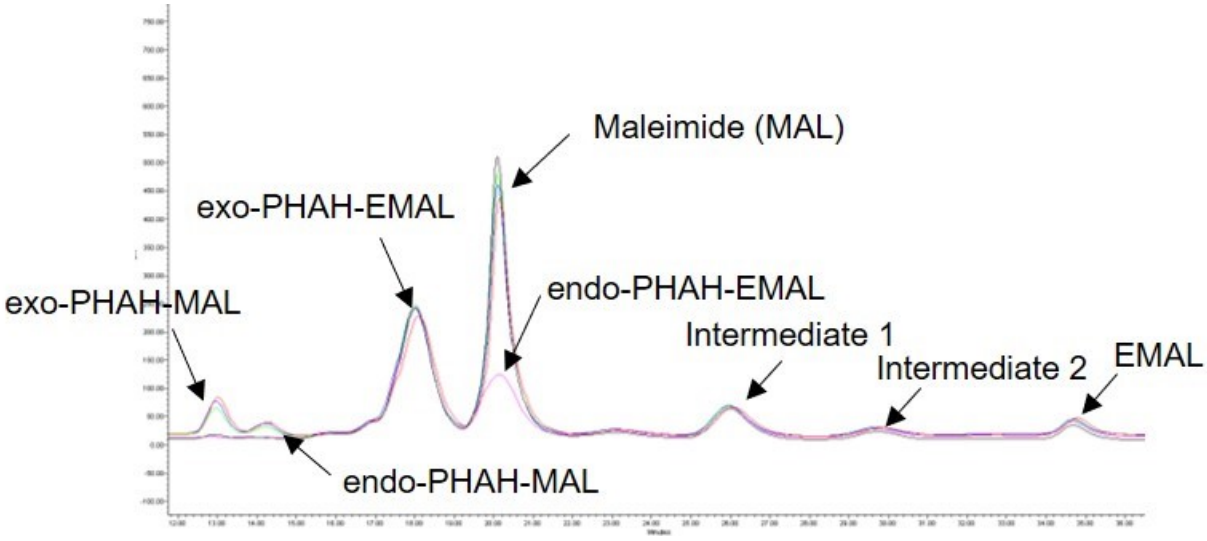

Figure S1. HPLC analysis for maleimide exchange at pH 5.0; After retro Diels-Alder reaction of PHAH-EMAL at 37℃ for 68 h, samples were collected by adding the maleimide (black) and carrying out Diels-Alder reaction at 22℃ for 1day (green), 2day (blue), and 3day (red).

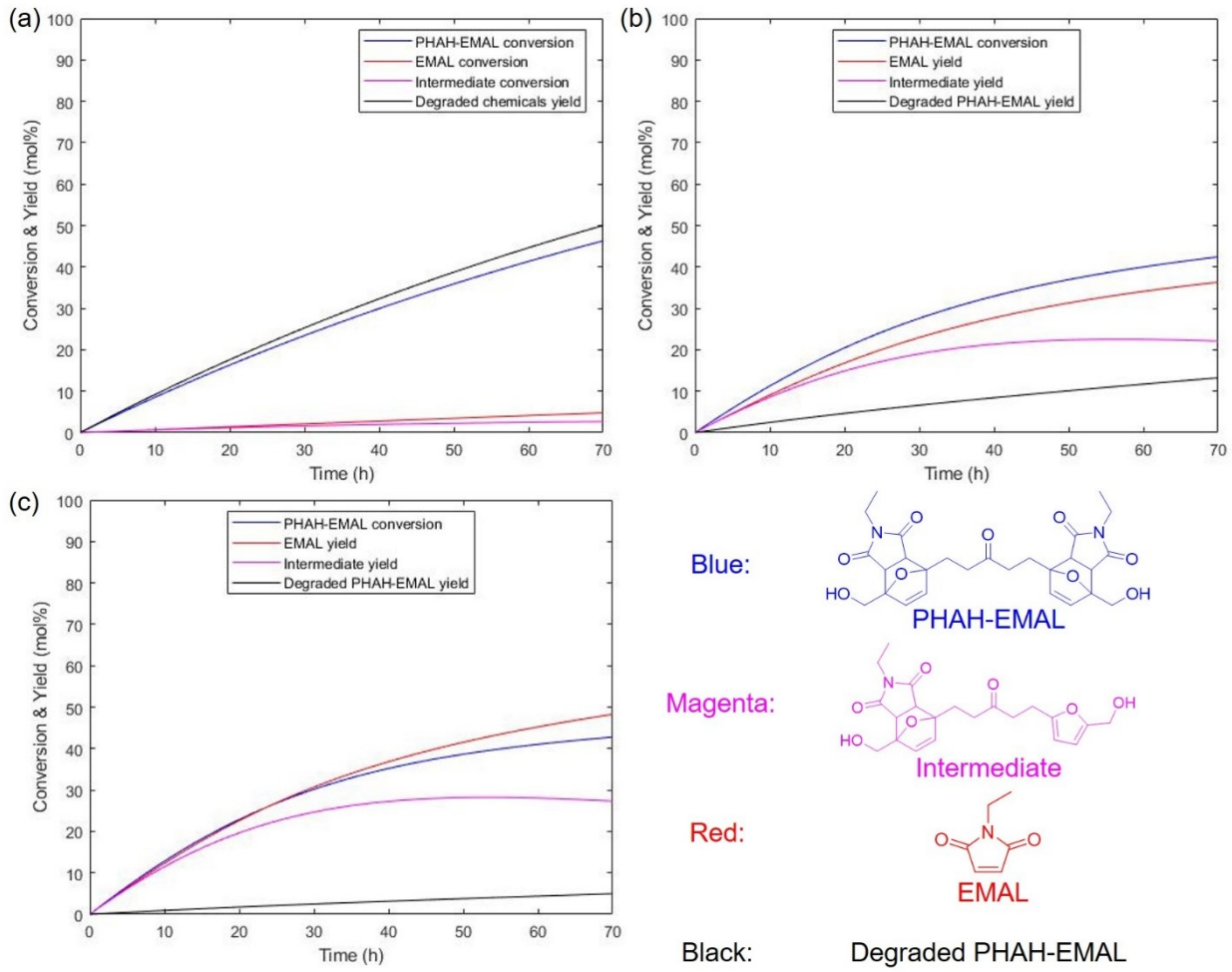

Figure S2. Simulation of reaction kinetics for the yield of EMAL at pharmacokinetic feed concentration ($[PHAH\text{-}EMAL]_0$=256 μg/mL=0.92 mM) under (a) pH7.4, (b) pH6.0, and (c) pH5.0 at 37℃ in biological broth.

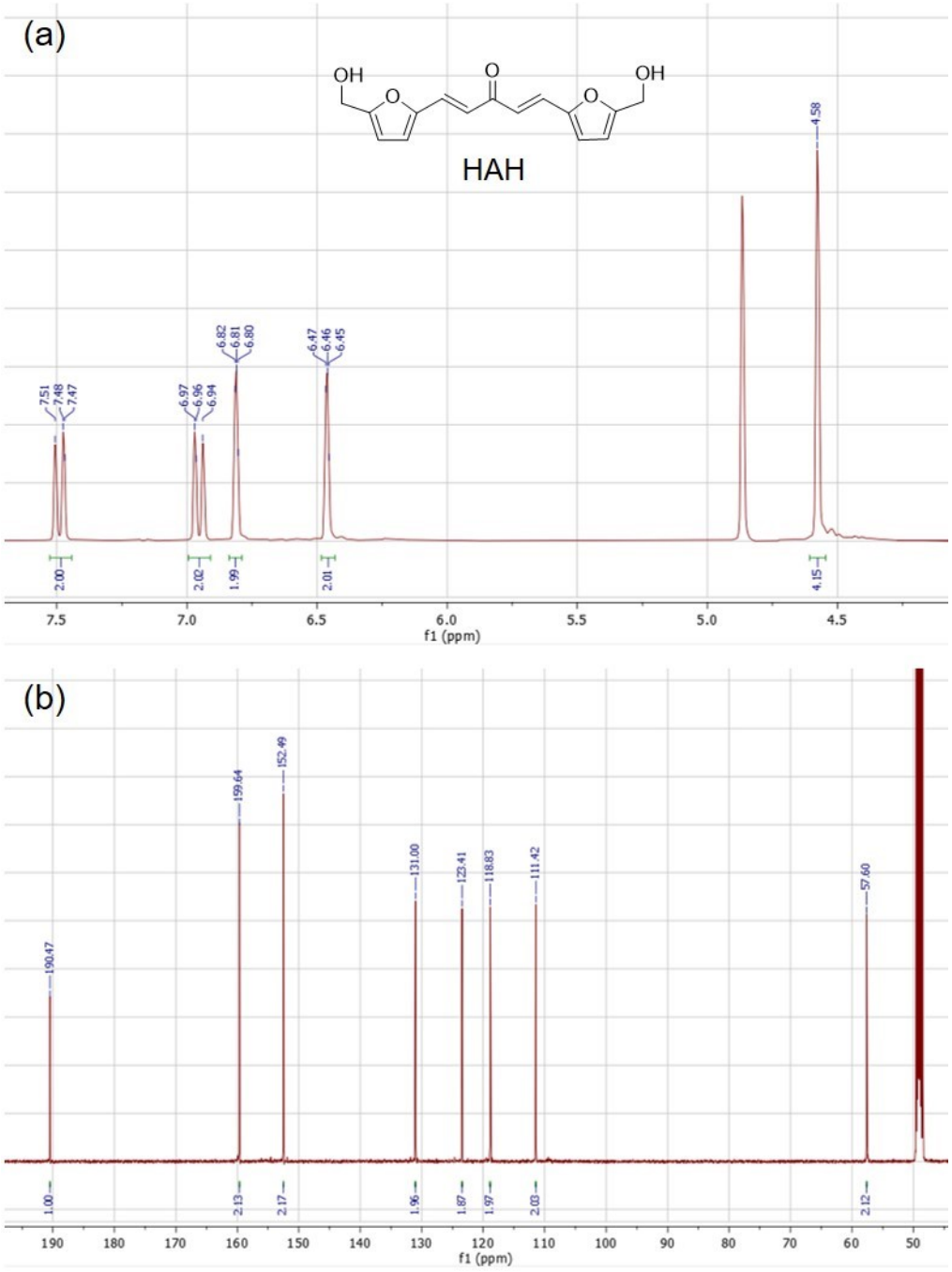

Figure S3. (a) ^{1}H NMR and (b) ^{13}C qNMR of HAH by aldol-condensation of HMF and acetone. ^{1}H NMR: (500 MHz, MeOD) δ: 7.57 (1H), 7.48 (1H), 6.97 (1H), 6.94 (1H), 6.82-6.80 (2H), 6.47-6.45 (2H), 4.58 (4H) ppm, ^{13}C qNMR: (126 MHz, MeOD) δ: 190.47 (1C), 159.67 (2C), 152.49 (2C), 131.00 (2C), 123.41 (2C), 118.83 (2C), 111.42 (2C), 57.60 (2C) ppm.

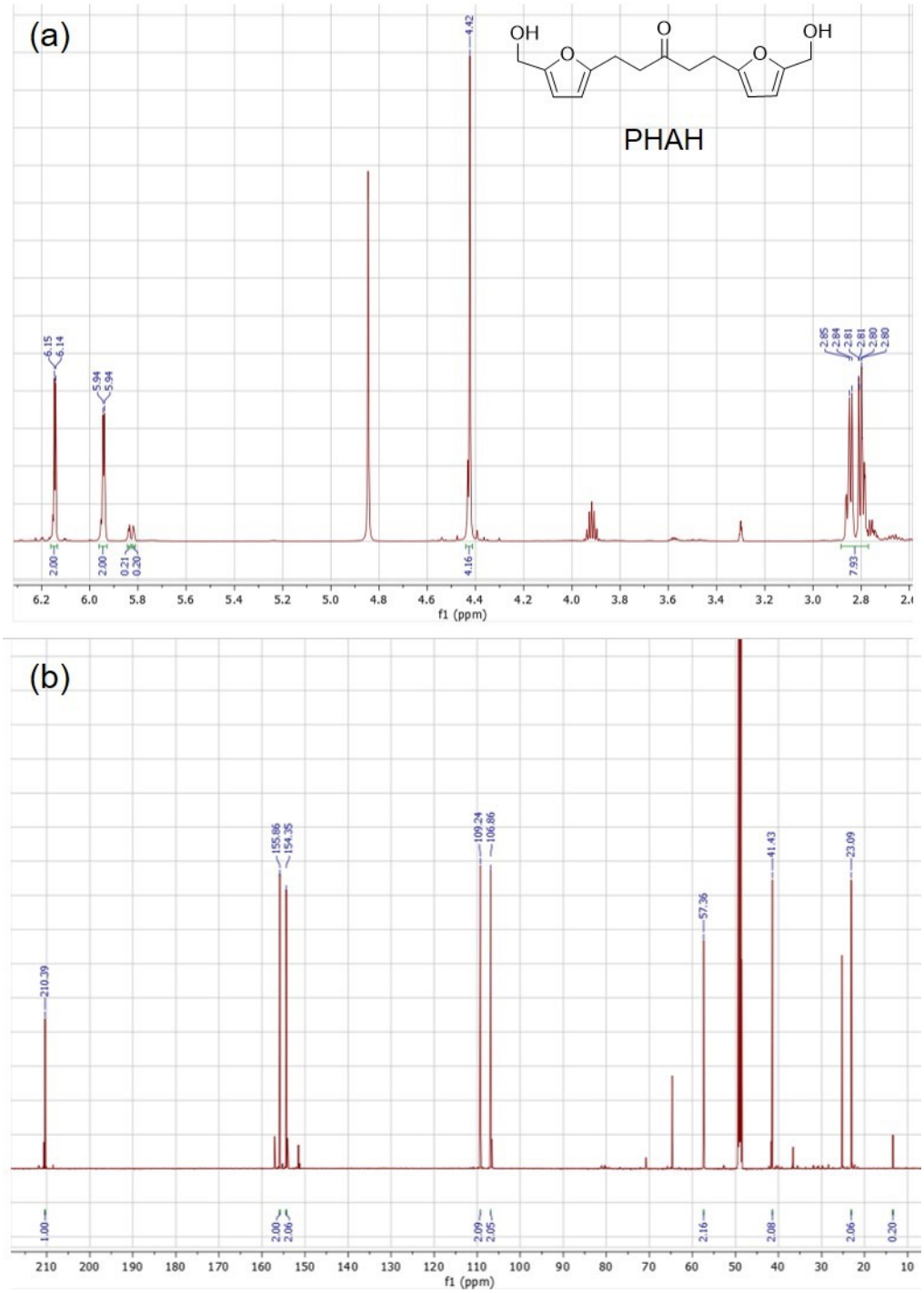

Figure S4. (a) ^{1}H NMR and (b) ^{13}C qNMR of PHAH by HAH hydrogenation over Cu/γ-Al_2O_3. ^{1}H NMR: (500 MHz, MeOD) δ 6.15 (d, 2H), 5.94 (d, 2H), 4.42 (s, 4H), 2.85-2.80 (m, 8H) ppm, ^{13}C qNMR (126 MHz, MeOD) δ 210.39 (1C), 155.86 (2C), 154.35 (2C), 109.24 (2C), 106.86 (2C), 57.39 (2C), 41.43 (2C), 23.09 (2C) ppm.

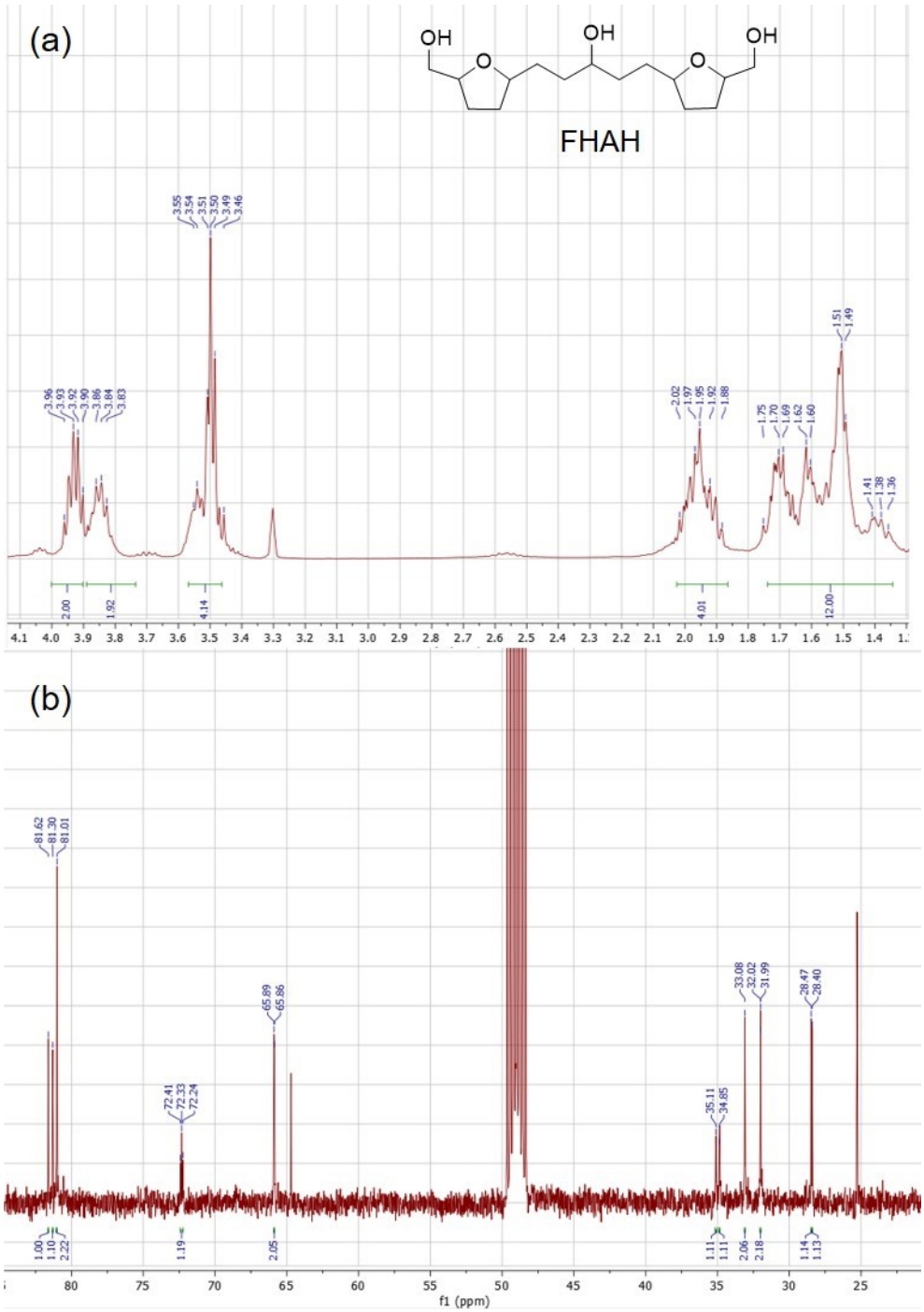

Figure S5. (a) ^{1}H NMR and (b) ^{13}C qNMR of FHAH by HAH hydrogenation over Ru/C. ^{1}H NMR: (500 MHz, MeOD) δ 3.96-3.90 (m, 2H), 3.90-3.83 (m, 2H), 3.55-3.46 (m, 4H), 2.02-1.88 (m, 4H), 1.75-1.36 (m, 12H) ppm, ^{13}C qNMR (126 MHz, MeOD) δ 81.62 (1C), 81.30 (1C), 81.01 (2C), 72.41-72.24 (1C), 65.89-65.86 (2C), 35.11-34.85 (2C), 33.08 (2C), 32.02-31.99 (2C), 28.47-28.40 (2C) ppm (Splits of ^{13}C chemical shifts resulted from diastereoisomers).

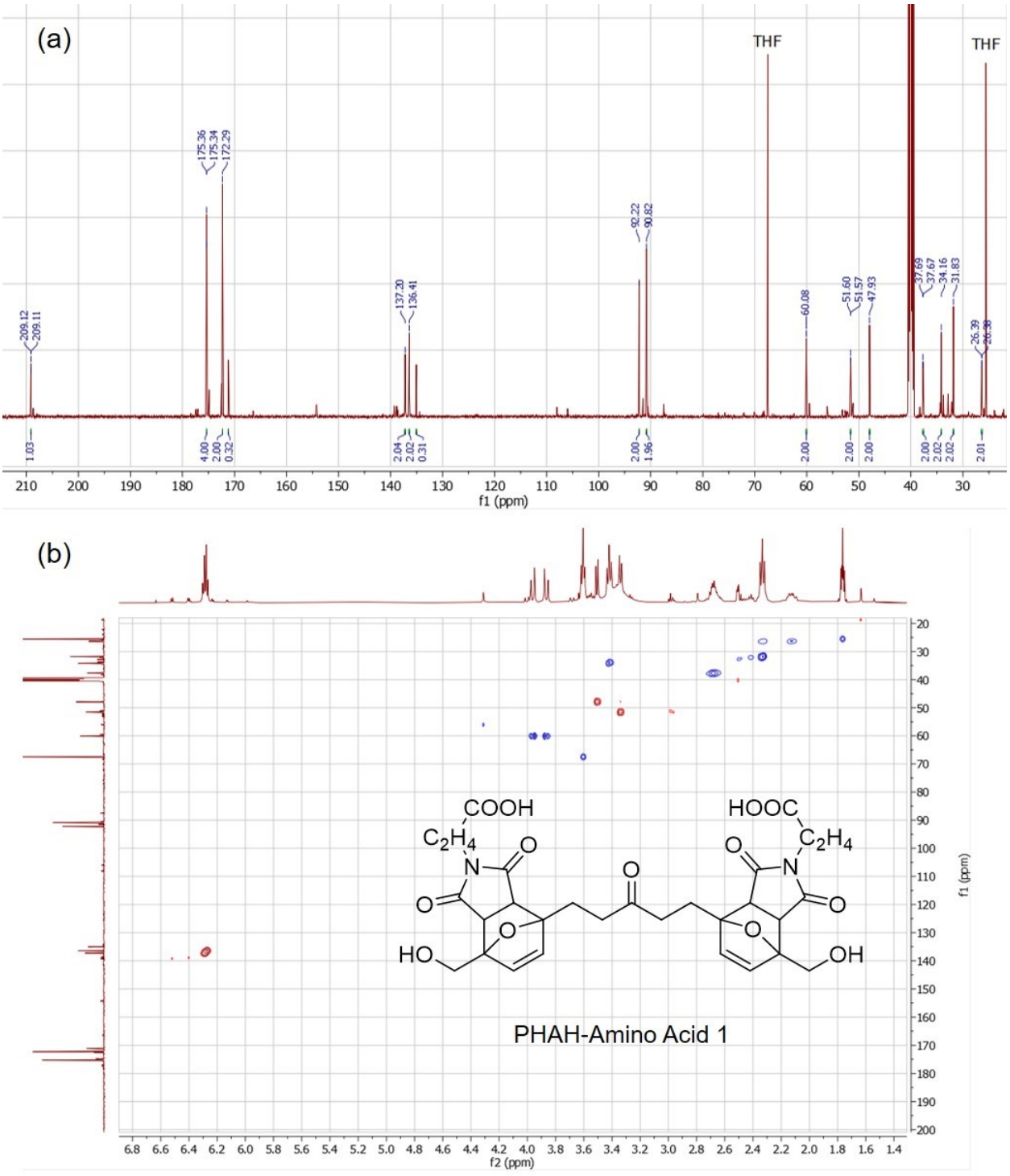

Figure S6. Characterization of PHAH-Amino Acid 1 (Amino acid 1 represents 3-Maleimidopropionic acid) by (a) ^{13}C qNMR and (b) 2D HSQC NMR spectrum (Red dot: -CH_3 and ≡CH group, Blue dot: =CH_2 group, Deuterated solvent: DMSO-d_6).

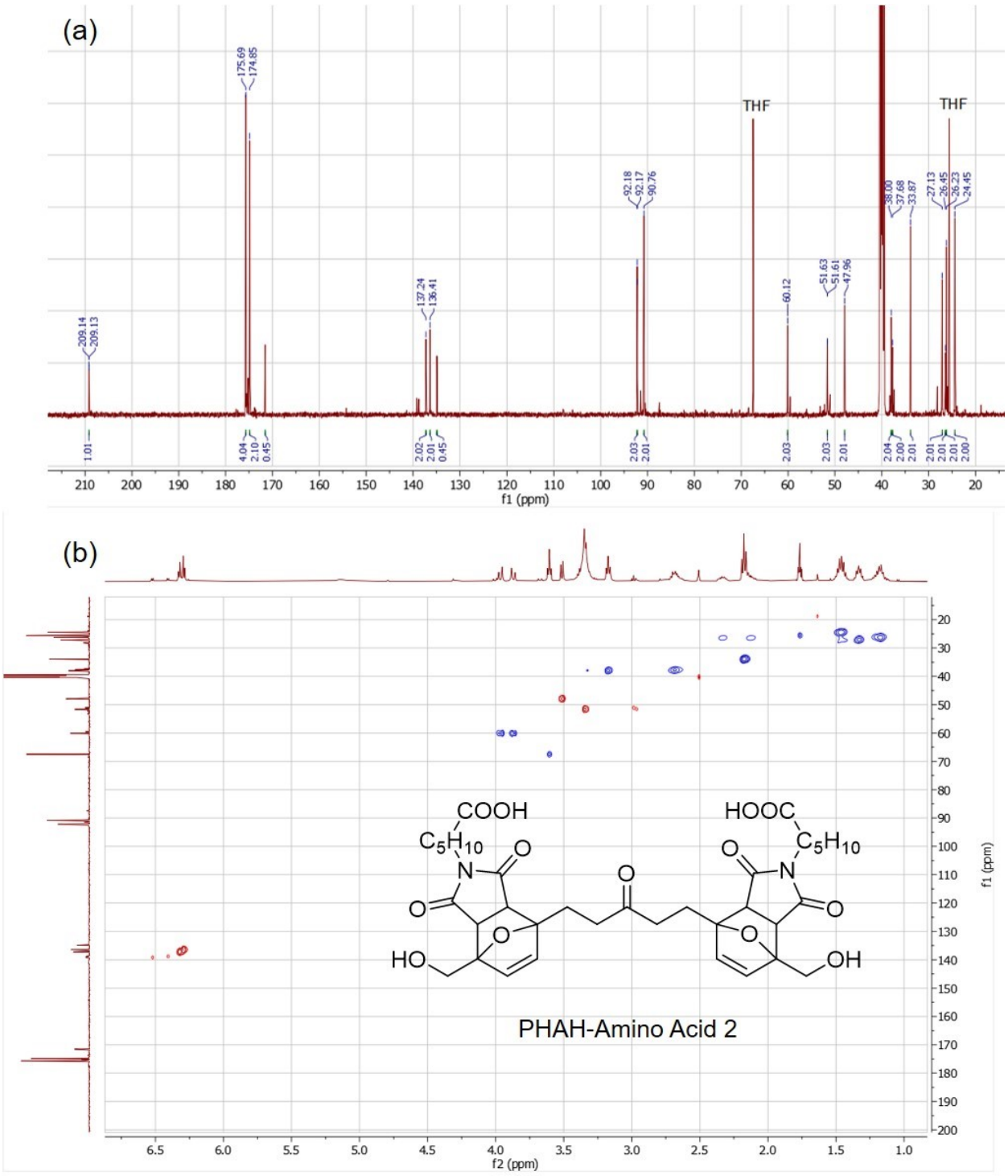

Figure S7. Characterization of PHAH-Amino Acid 2 (Amino acid 2 represents 6-Maleimidohexanoic acid) by (a) ^{13}C qNMR and (b) 2D HSQC NMR spectrum (Red dot: -CH_3 and ≡CH group, Blue dot: =CH_2 group, Deuterated solvent: DMSO-d_6).

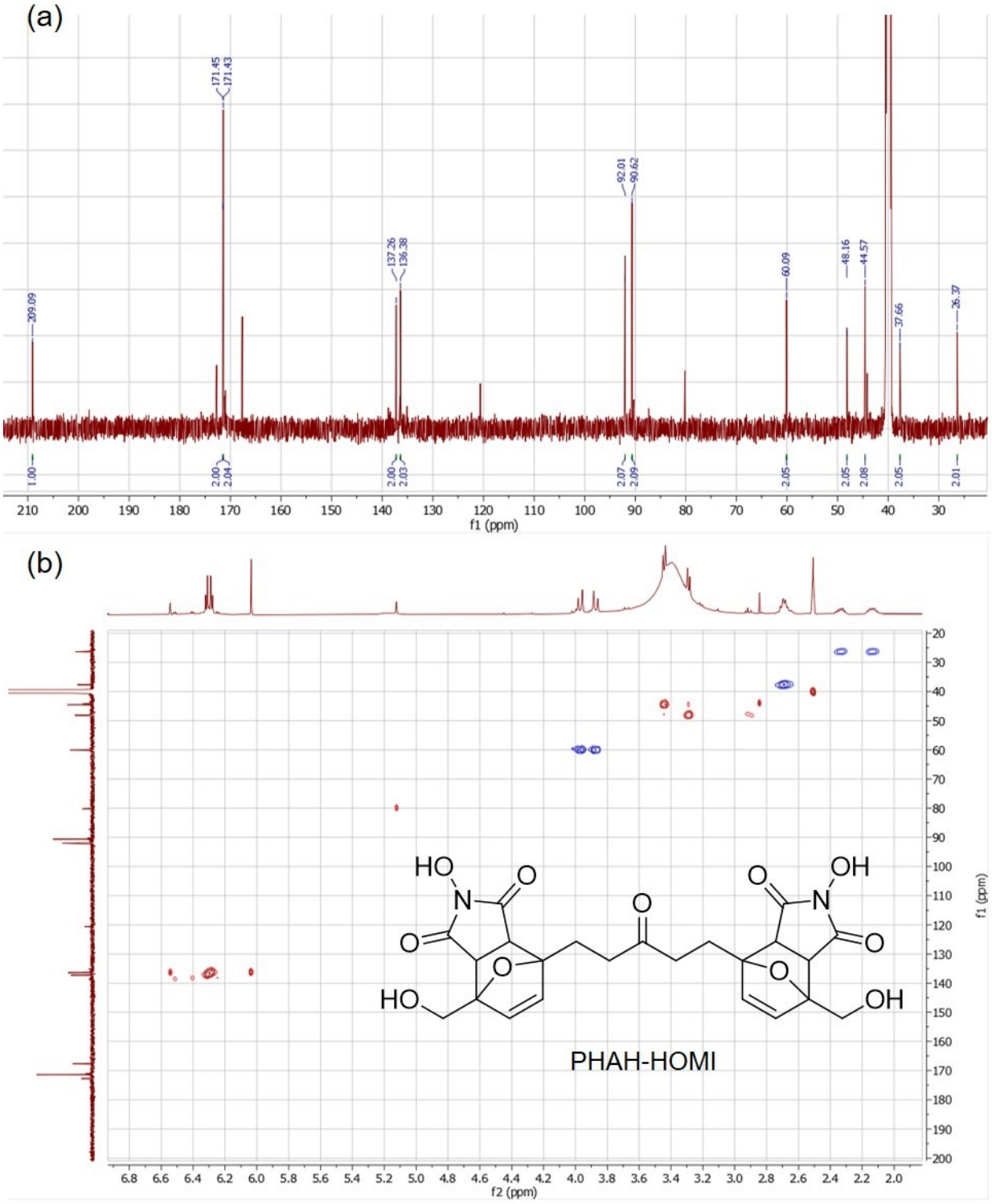

Figure S8. Characterization of PHAH-HOMI (HOMI represents N-Hydroxymaleimide) by (a) ^{13}C qNMR and (b) 2D HSQC NMR spectrum (Red dot: -CH_3 and ≡CH group, Blue dot: =CH_2 group, Deuterated solvent: DMSO-d_6).

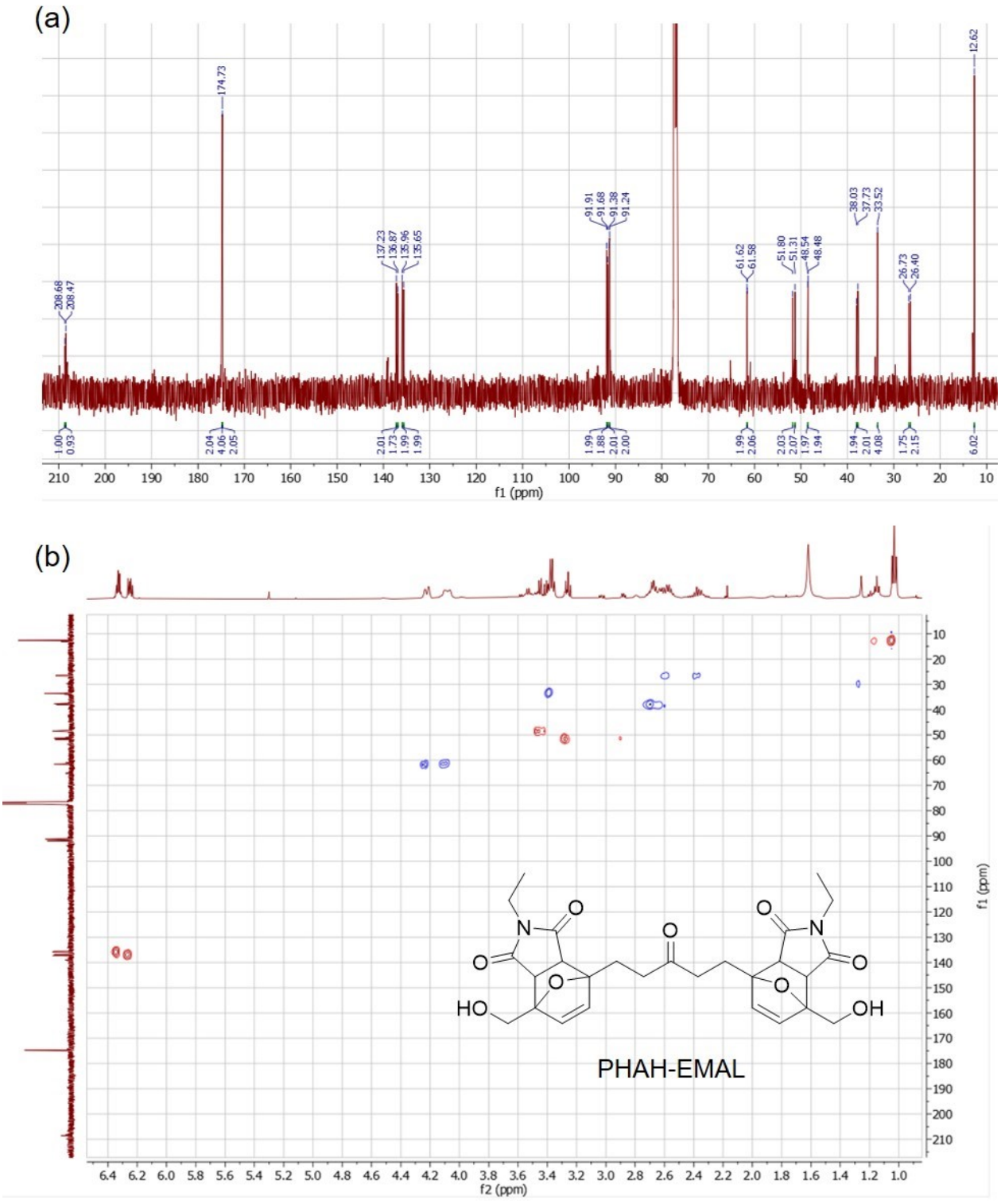

Figure S9. Characterization of PHAH-EMAL (EMAL represents N-ethyl maleimide) by (a) ^{13}C qNMR and (b) 2D HSQC NMR spectrum (Red dot: -CH_3 and ≡CH group, Blue dot: =CH_2 group, Deuterated solvent: DMSO-d_6).

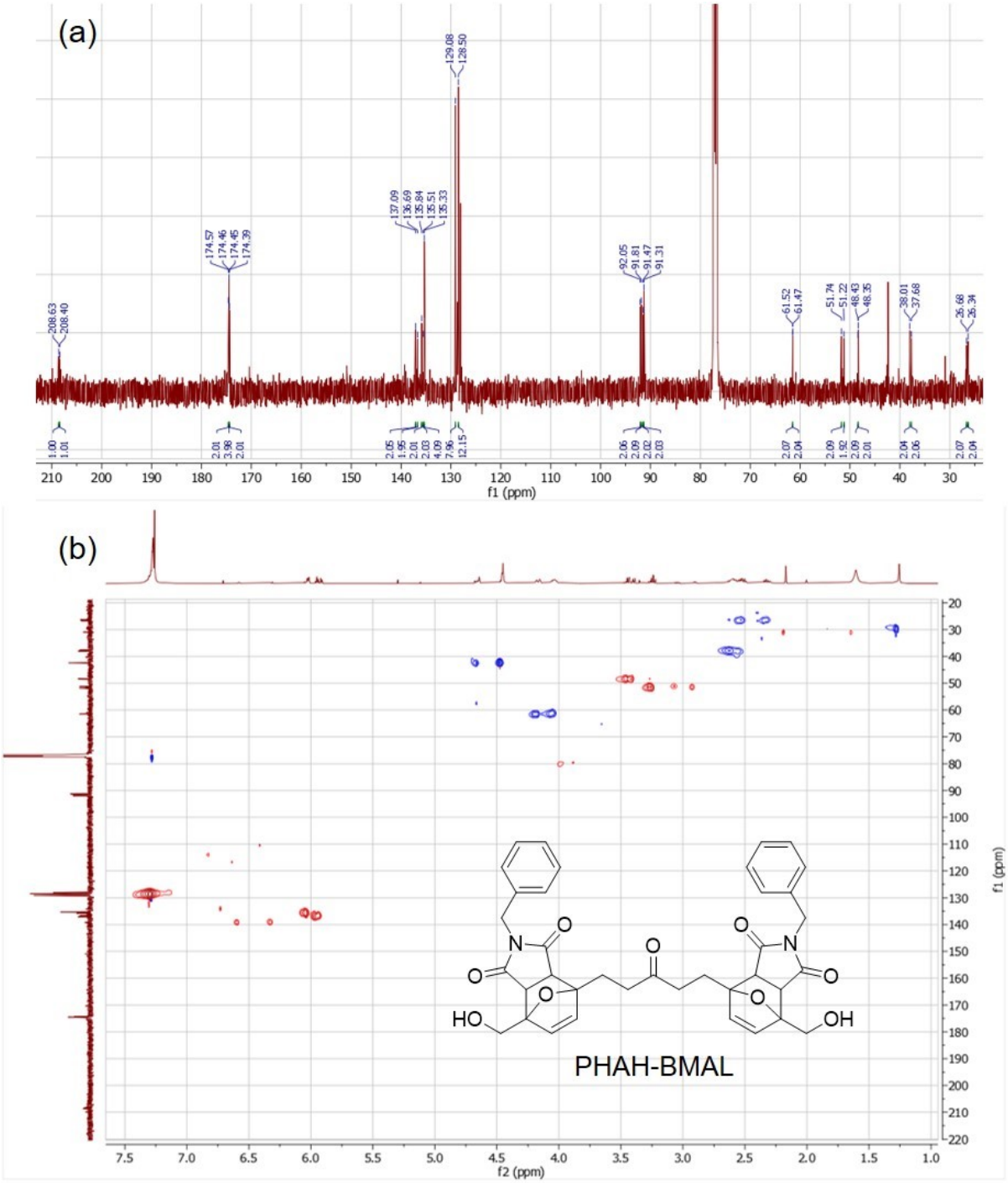

Figure S10. Characterization of PHAH-BMAL (BMAL represents N-benzyl maleimide) by (a) ^{13}C qNMR and (b) 2D HSQC NMR spectrum (Red dot: -CH_3 and ≡CH group, Blue dot: =CH_2 group, Deuterated solvent: $CDCl_3$), Split chemical shifts in ^{13}C qNMR resulted from endo- and exo- isomers.

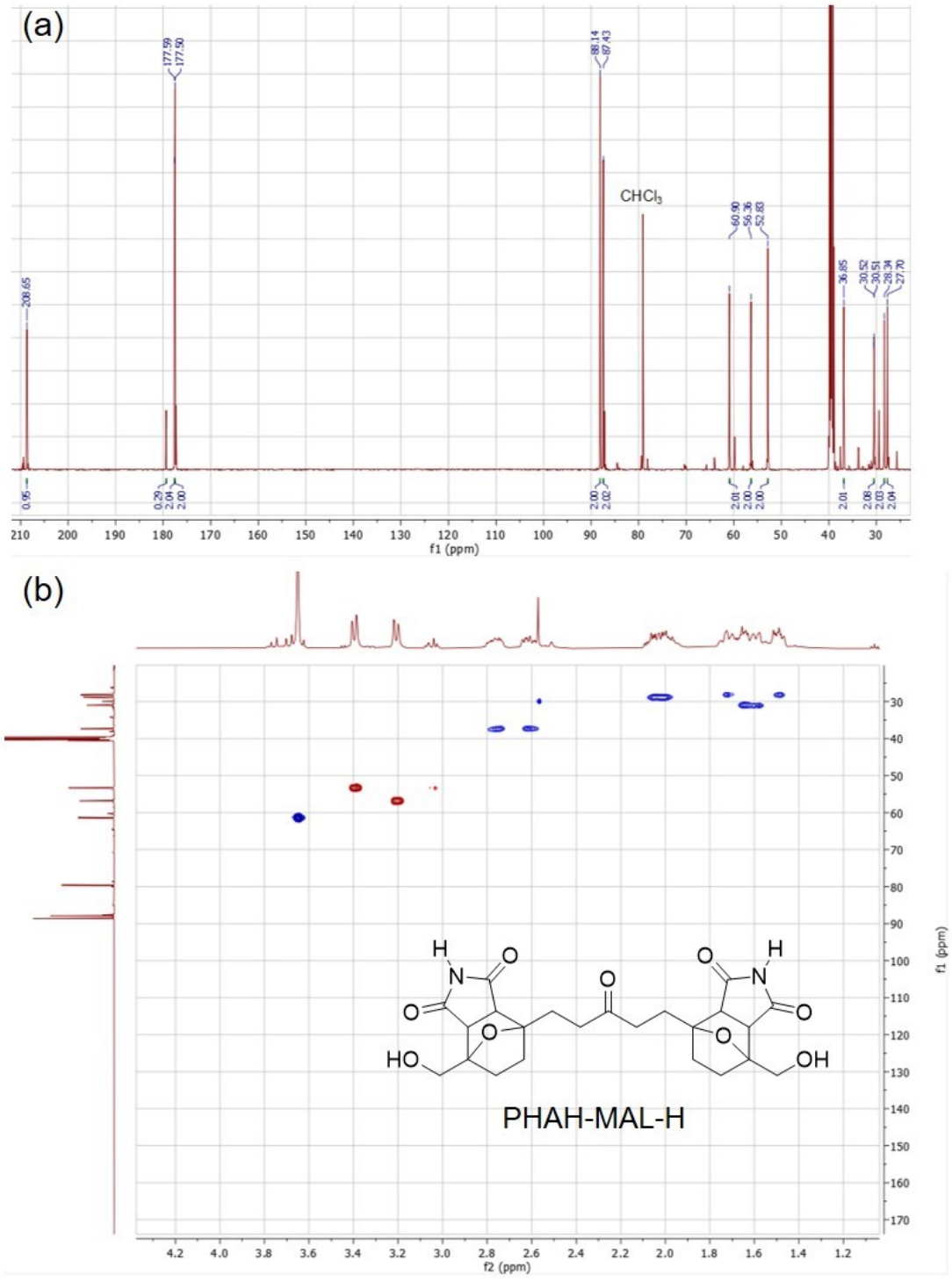

Figure S11. Characterization of PHAH-MAL-H (Hydrogenated PHAH-MAL) by (a) ^{13}C qNMR and (b) 2D HSQC NMR spectrum (Red dot: -CH_3 and ≡CH group, Blue dot: =CH_2 group, Deuterated solvent: DMSO-d_6).

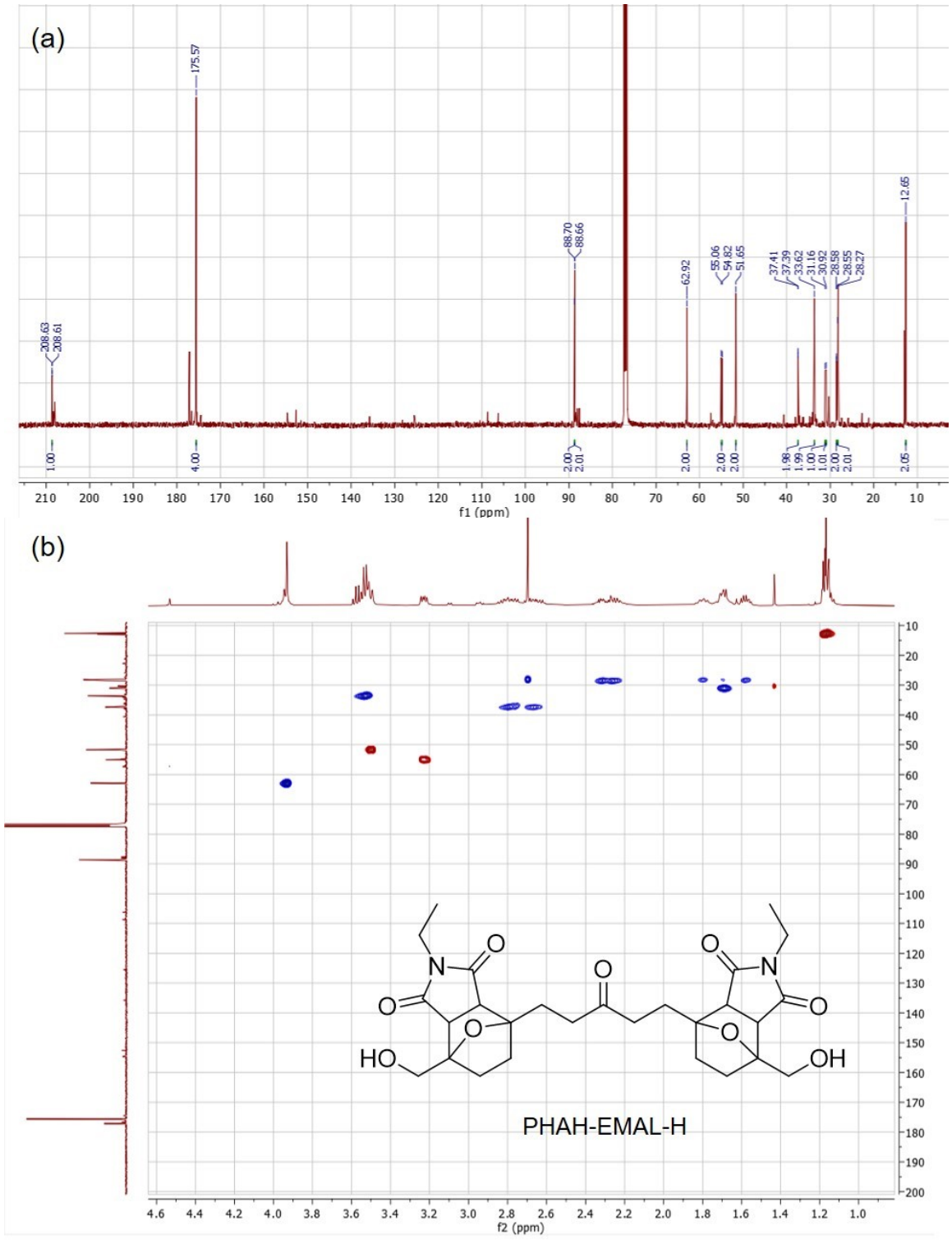

Figure S12. Characterization of PHAH-EMAL-H (Hydrogenated PHAH-EMAL) by (a) ^{13}C qNMR and (b) 2D HSQC NMR spectrum (Red dot: -CH_3 and ≡CH group, Blue dot: =CH_2 group, Deuterated solvent: $CDCl_3$).

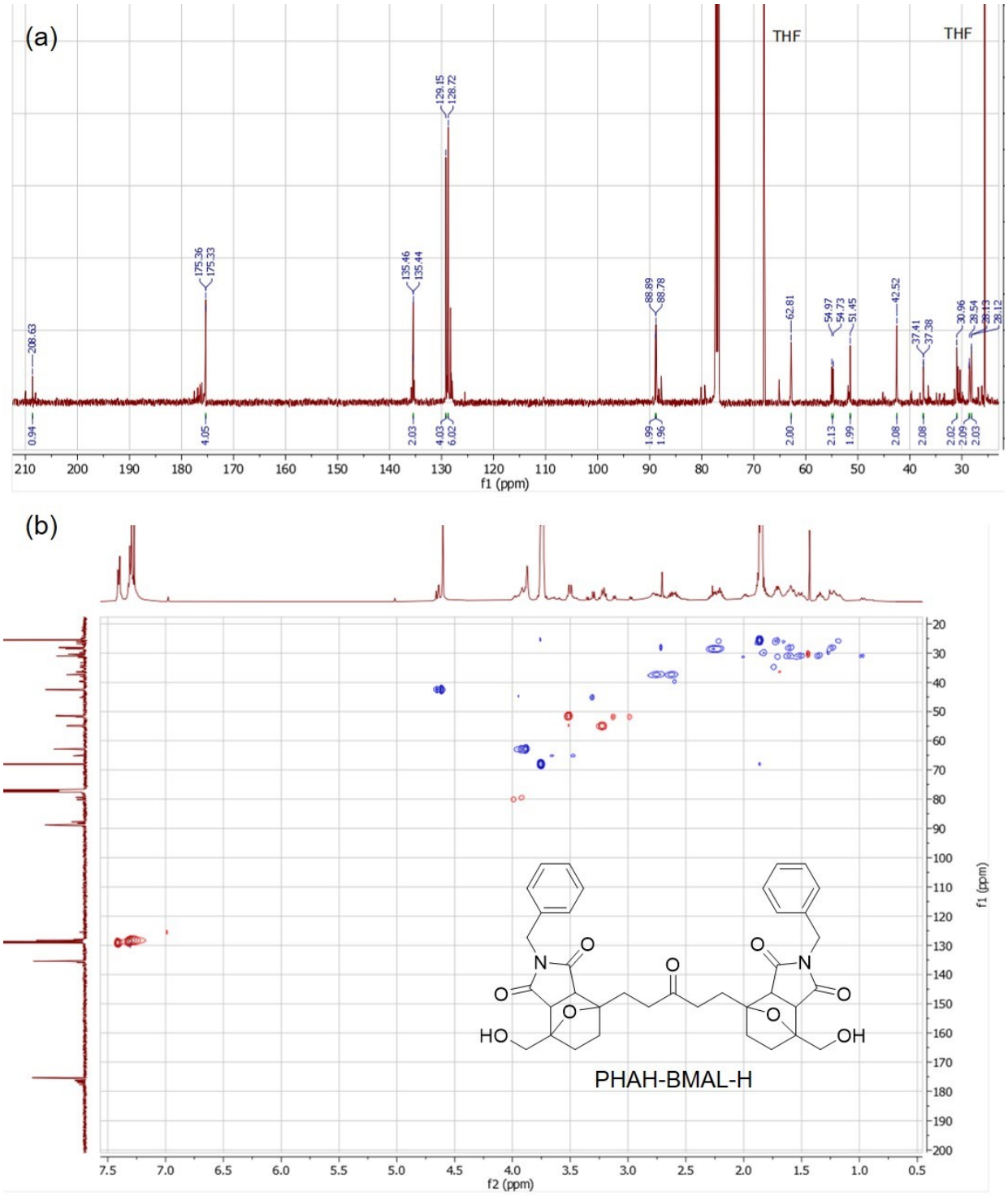

Figure S13. Characterization of PHAH-BMAL-H (Hydrogenated PHAH-BMAL) by (a) ^{13}C qNMR and (b) 2D HSQC NMR spectrum (Red dot: -CH_3 and ≡CH group, Blue dot: =CH_2 group, Deuterated solvent: $CDCl_3$).

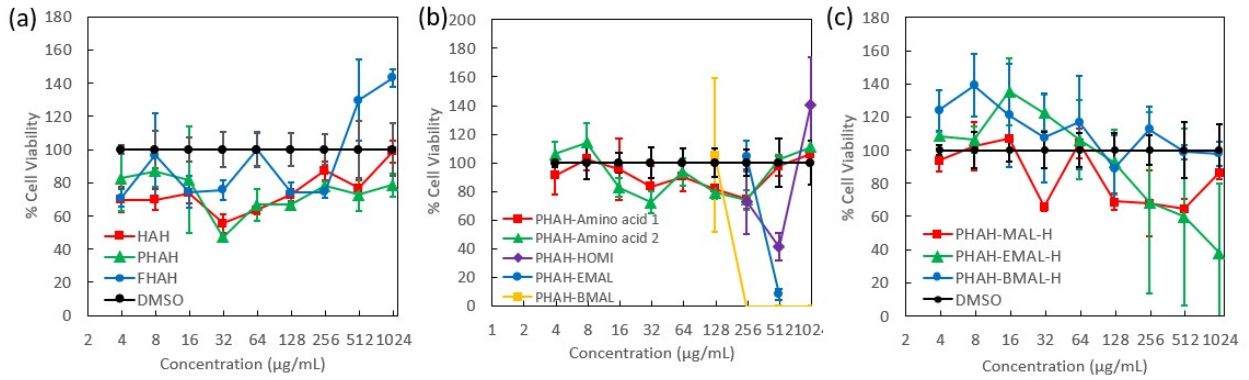

Figure S14. Plots of concentration-dependent growth inhibition of *C. albicans* by compounds. *C. albicans* cells (5×10^3 cells/mL) were incubated with compounds for 48 h and susceptibility was assessed using an XTT reduction assay to compare the absorbance at 490 nm for compound-treated samples and untreated samples. Data points are the average of at least two technical replicates each and error bars represent the standard deviation. Graphs are shown for (a) Entries 1-3, (b) Entries 4-8, (c) Entries 9-11. Each viability curve was normalized against a DMSO vehicle control, shown in black circles.

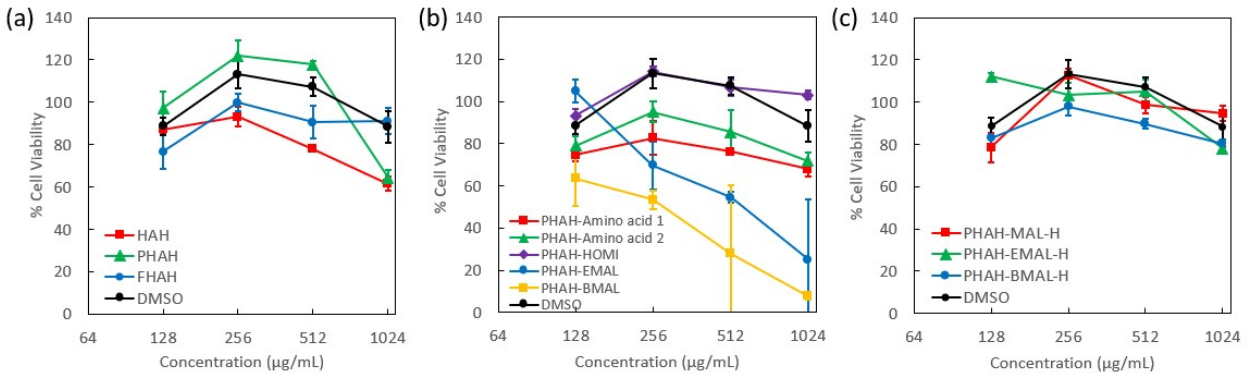

Figure S15. Plots of concentration-dependent growth inhibition of *S. aureus* by compounds. *S. aureus* cells (10^6 cells/mL) were incubated with compounds for 24 h and susceptibility was assessed using an XTT reduction assay to compare the absorbance at 490 nm for compound-treated samples and untreated samples. Data points are the average of at least two technical replicates each and error bars represent the standard deviation. Graphs are shown for (a) Entries 1-3, (b) Entries 4-8, (c) Entries 9-11. DMSO vehicle controls were added as comparison.

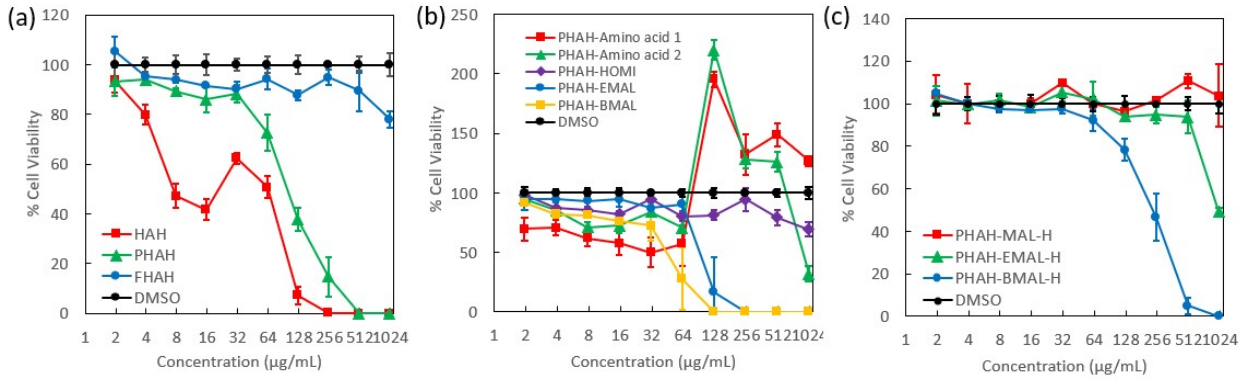

Figure S16. Characterization of cytotoxicity against MDA-MB-231 triple-negative human breast cancer cells. MDA-MB-231 cells were seeded at (25,000 cells/mL) for 24 h and then incubated with compounds for 48 h and cytotoxicity was assessed using an ATP luminescence assay (CellTiterGlo 2.0) to compare the luminescence for compound-treated samples and untreated samples. Data points are the average of at least two technical replicates each and error bars represent the standard deviation. Graphs are shown for (a) Entries 1-3, (b) Entries 4-8, (c) Entries 9-11. Each viability curve was normalized against a DMSO vehicle control, shown in black circles.

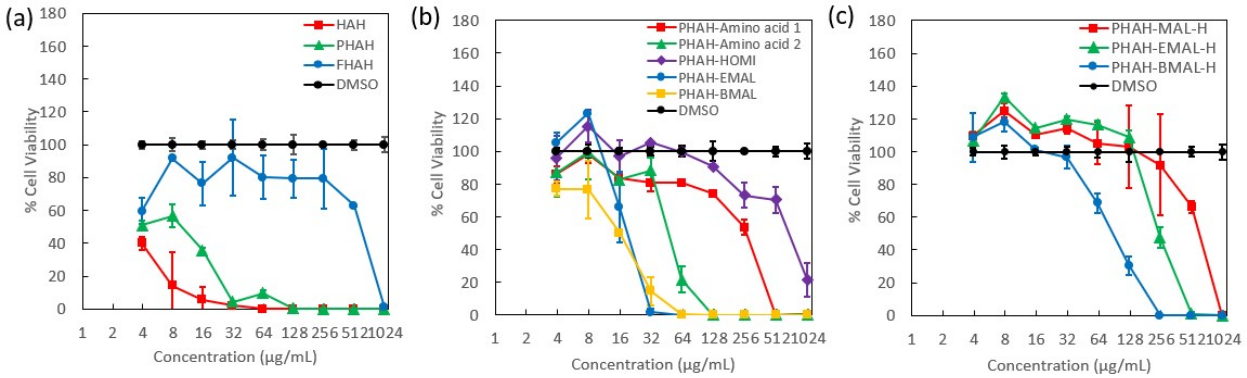

Figure S17. Characterization of cytotoxicity against MCF-10A human mammary epithelial cells. MCF-10A cells were seeded at (25,000 cells/mL) for 24 h and then incubated with compounds for 48 h and cytotoxicity was assessed using an ATP luminescence assay (CellTiterGlo 2.0) to compare the luminescence for compound-treated samples and untreated samples. Data points are the average of at least two technical replicates each and error bars represent the standard deviation. Graphs are shown for (a) Entries 1-3, (b) Entries 4-8, (c) Entries 9-11. Each viability curve was normalized against a DMSO vehicle control, shown in black circles.

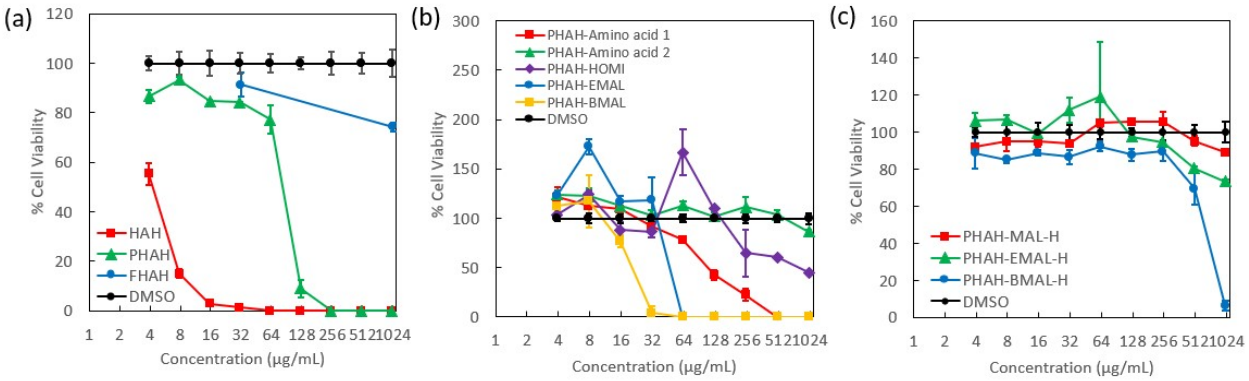

Figure S18. Characterization of cytotoxicity against NIH-3T3 mouse fibroblast cells. NIH-3T3 cells were seeded at (25,000 cells/mL) for 24 h and then incubated with compounds for 48 h and cytotoxicity was assessed using an ATP luminescence assay (CellTiterGlo 2.0) to compare the luminescence for compound-treated samples and untreated samples. Data points are the average of at least two technical replicates each and error bars represent the standard deviation. Graphs are shown for (a) Entries 1-3, (b) Entries 4-8, (c) Entries 9-11. Each viability curve was normalized against a DMSO vehicle control, shown in black circles.

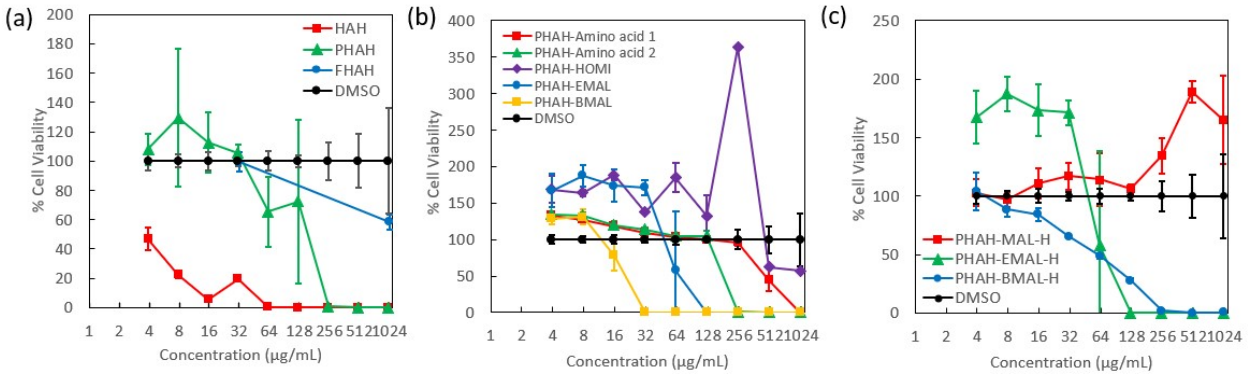

Figure S19. Characterization of cytotoxicity against human umbilical vein endothelial cells (HUVECs). HUVECs were seeded at (25,000 cells/mL) for 24 h and then incubated with compounds for 48 h and cytotoxicity was assessed using an ATP luminescence assay (CellTiterGlo 2.0) to compare the luminescence for compound-treated samples and untreated samples. Data points are the average of at least two technical replicates each and error bars represent the standard deviation. Graphs are shown for (a) Entries 1-3, (b) Entries 4-8, (c) Entries 9-11. Each viability curve was normalized against a DMSO vehicle control, shown in black circles.

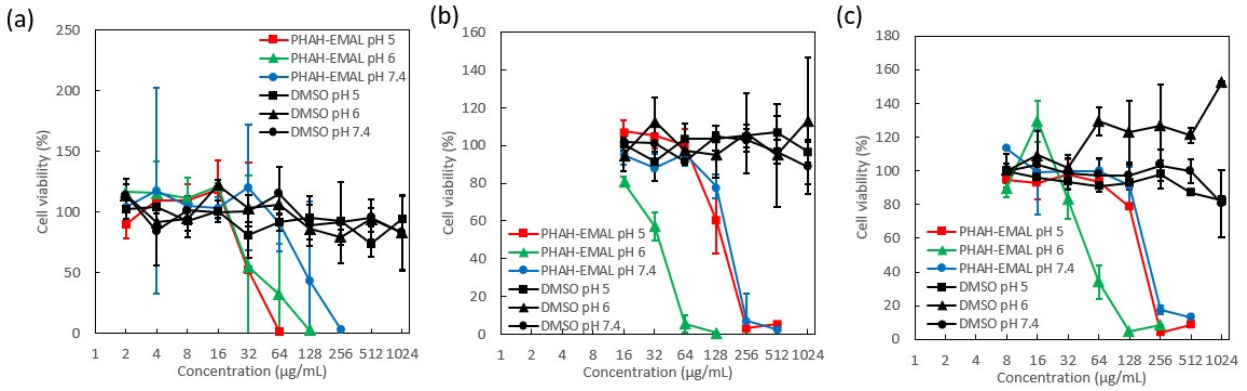

Figure S20. pH-dependent antifungal MIC characterization assay of PHAH-EMAL against *C. albicans*. *C. albicans* cells (5×10^3 cells/mL) were incubated with compounds for 48 h in different pH broth (RPMI 1640 buffered with citrate-phosphate to adjust pH) and susceptibility was assessed using an XTT reduction assay to compare the absorbance at 490 nm for compound-treated samples and untreated samples. Data points are the average of at least two technical replicates each and error bars represent the standard deviation. Graphs are shown for (a) Trial 1, (b) Trial 2, and (c) Trial 3. DMSO vehicle controls at different pH were added as negative controls.

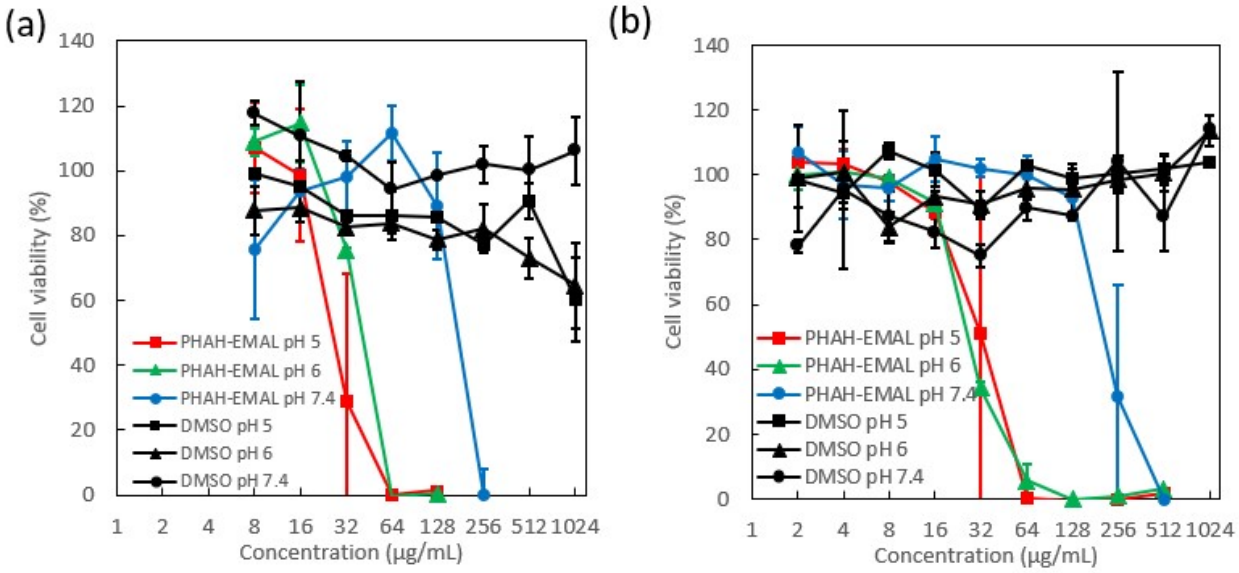

Figure S21. pH-dependent antifungal MIC characterization assay of PHAH-EMAL against *C. parapsilosis*. *C. parapsilosis* cells (5×10^3 cells/mL) were incubated with compounds for 48 h in different pH broth (RPMI 1640 buffered with citrate-phosphate to adjust pH) and susceptibility was assessed using an XTT reduction assay to compare the absorbance at 490 nm for compound-treated samples and untreated samples. Data points are the average of at least two technical replicates each and error bars represent the standard deviation. Graphs are shown for (a) Trial 1 and (b) Trial 2. DMSO vehicle controls at different pH were added as negative controls.

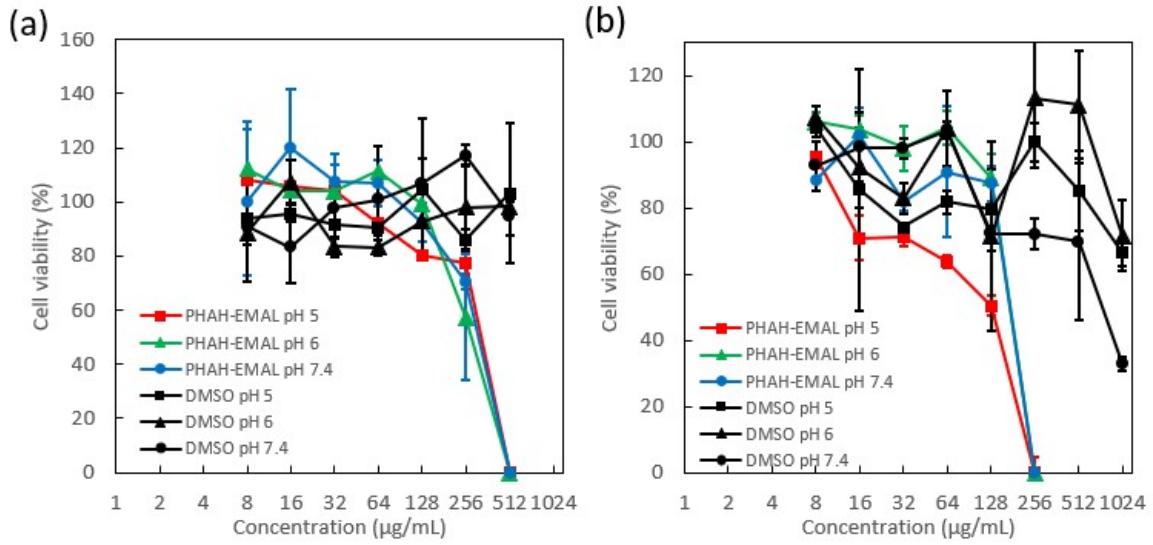

Figure S22. pH-dependent antifungal MIC characterization assay of PHAH-EMAL against *C. tropicalis*. *C. tropicalis* cells (5×10^3 cells/mL) were incubated with compounds for 48 h in different pH broth (RPMI 1640 buffered with citrate-phosphate to adjust pH) and susceptibility was assessed using an XTT reduction assay to compare the absorbance at 490 nm for compound-treated samples and untreated samples. Data points are the average of at least two technical replicates each and error bars represent the standard deviation. Graphs are shown for (a) Trial 1 and (b) Trial 2. DMSO vehicle controls at different pH were added as negative controls.

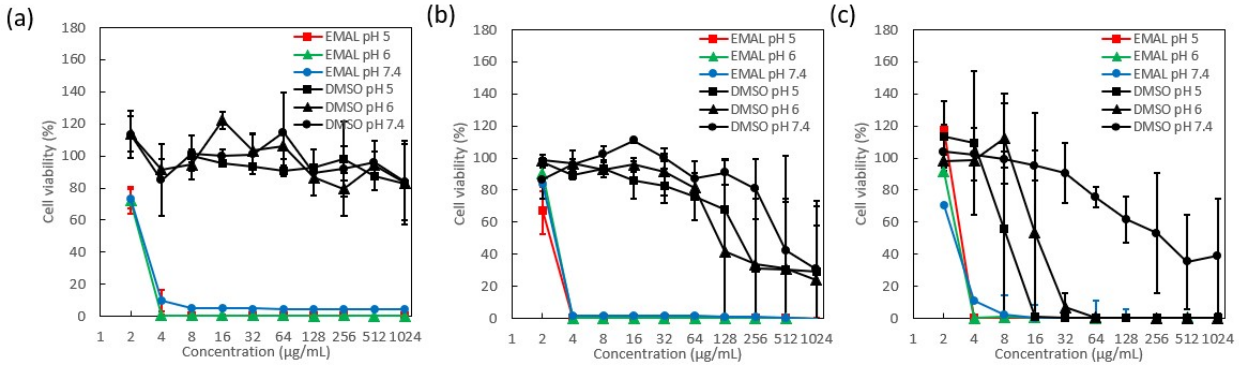

Figure S23. pH-dependent antifungal MIC characterization assay of EMAL against *C. albicans, C. tropicalis, and C. parapsilosis*. Cells (5×10^3 cells/mL) were incubated with compounds for 48 h in different pH broth (RPMI 1640 buffered with citrate-phosphate to adjust pH) and susceptibility was assessed using an XTT reduction assay to compare the absorbance at 490 nm for compound-treated samples and untreated samples. Data points are the average of at least two technical replicates each and error bars represent the standard deviation. Graphs are shown for (a) *C. albicans*, (b) *C. tropicalis*, and (c) *C. parapsilosis*. DMSO vehicle controls at different pH were added as negative controls.

Table S1. The mean values of the regressed rate constants for Diels-Alder, retro Diels-Alder, and degradation under different pH conditions at 37°C in biological broth.

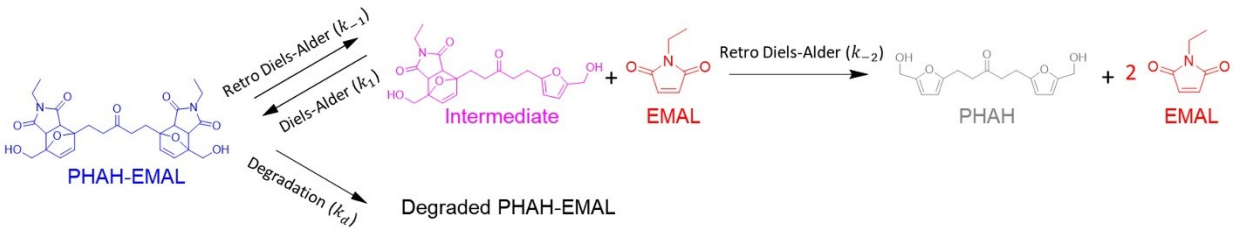

pH	k_{-1} (h^{-1})	k_1 ($mM^{-1}h^{-1}$)	k_{-2} (h^{-1})	k_d (h^{-1})	$(k_{-1}+k_{-2})/k_d$	$(k_{-1}+k_{-2})/k_1$ (mM)
7.4	0.0007	0.0206	0.0092	0.0096	0.85	0.41
6.0	0.0095	0.0646	0.0059	0.0026	5.92	0.24
5.0	0.0130	0.0535	0.0068	0.0010	19.8	0.37

Table S2. The composition of RPMI 1640 Broth with citrate-phosphate buffer at different pH.

pH	Molar Concentration (M)	
	Disodium Phosphate (Na_2HPO_4)	Citric Acid
5.0	0.103	0.049
6.0	0.126	0.037
7.4	0.181	0.009